JOURNAL OF MATERIALS SCIENCE 40 (2005) 3383 – 3393

Identification and characterization of diffusion barriers for Cu/SiC systems

GLENN SUNDBERG*
Department of Engineering Technology, University of Massachusetts, Lowell; Center for Advanced Materials, Department of Chemical and Nuclear Engineering, University of Massachusetts, Lowell
E-mail: glenn_sundberg@uml.edu

PRADEEP PAUL, CHANGMO SUNG, THOMAS VASILOS
Center for Advanced Materials, Department of Chemical and Nuclear Engineering, University of Massachusetts, Lowell

The promise of CuSiC metal matrix composites (MMCs) as a thermal management material is to provide increased power density and high reliability for advanced electronic systems. CuSiC will offer high thermal conductivity between 250 and 325 W/mK with corresponding adjustable thermal expansion coefficient between 8.0 and 12.5 ppm/°C. The major challenge in development of these materials is control of the interface interactions. Cu and SiC react at high temperatures between 850 and 1150°C, needed for fabrication of the CuSiC material, with an expected decrease in thermal conductivity of the CuSiC MMCs as the Si product of reaction dissolves into the Cu.

The application of barrier coatings onto SiC was observed to control chemical reaction of Cu and SiC. In the current study, the effectiveness of four barriers to prevent Cu diffusion and reaction with SiC were evaluated between 850 to 1150°C. Immersion experiments were conducted at 1150°C to understand the reaction between copper and silicon carbide. Reaction products were identified with transmission electron microscopy (TEM) and electron diffraction. Laser flash thermal diffusivity measurements confirmed thermal conductivity to decrease with increasing silicon content of the copper as determined by induction coupled plasma mass spectrometry (ICPMS) and glow discharge mass spectrometry (GDMS). © *2005 Springer Science + Business Media, Inc.*

1. Introduction

In the past decade, Metal Matrix Composites (MMC's) have come into prominence by offering significant improvements over their polymer matrix counterparts due to increased: tolerance of high temperature, transverse strength, chemical stability, hardness and wear resistance, with significantly greater toughness and ductility than ceramic matrix composites [1]. For example, aluminum reinforced with Al_2O_3 and SiO_2 is used in the aerospace, aircraft and automotive industries because of excellent thermo-physical properties such as relatively low coefficient of thermal expansion (CTE), high thermal conductivity, and improved mechanical properties [2]. The promise of a CuSiC metal matrix composite as a thermal management material is to enable increased power density and high reliability for advanced electronic systems. Theoretically, CuSiC should have a high thermal conductivity between 250 and 325 W/mK and corresponding adjustable thermal expansion coefficient between 8.0 and 12.5 ppm/°C. CuSiC used as a heat spreader in power electronics would achieve high transfer of heat to extend die life. Also, CuSiC with a CTE matched to the other materials in the electronic package would decrease stress in service minimizing failure to solder joints, wire bonds and die delamination/cracking. A CuSiC body would be compatible with CuAg eutectic brazing (CuSil) at ∼810°C, water based cooling systems (vapor chambers, heat pipes, cold-plates) and allow integration of high thermal conductivity materials, such as diamond and thermal pyrolytic graphite (TPG) into the CuSiC structure.

Properties of such materials are often limited by interface phenomena [3]. The matrix reinforcement interface can suffer from the coefficient of thermal expansion (CTE) mismatch, mechanical incompatibility and thermodynamic instability [4]. Thermodynamic instability is due to the reactive nature of the interface between dissimilar materials used for the continuous matrix and the particle reinforcement. These materials often represent highly non-equilibrium systems which suffer from high chemical reaction rates at elevated temperature. It has been shown for silicon die with

*Author to whom all correspondence should be addressed.

sputtered Cu for electrical interconnection that Cu diffuses easily into the interlayer dielectrics and silicon device to react with Si atoms to form Cu_3 Si compounds at fabrication temperatures (∼700°C) [5] . The authors of this study have observed SiC to react with copper between 965 and 1150°C resulting in silicon dissolving into Cu with a corresponding decrease in Cu thermal conductivity. Therefore, a barrier layer was thought to be essential to prevent the interfacial reactions between Cu and SiC. The literature has shown various diffusion barriers including refractory metal (Ta and W) [6, 7], nitrides (TiN and TaN) [8, 9] and compounds (TiW and Ta-Si-N) [10] have been used to passivate the interface between Si die and Cu electrical interconnects. In the current study the effectiveness of four barriers to prevent Cu transport at temperatures greater than 1050°C was investigated: physical vapor deposited (PVD) TiN, chemical vapor deposited (CVD) Diamond-like Carbon, and multilayer coatings of chemical vapor deposited CVD TiN/TiC/TiCN/TiN, and CVD TiN/TiC/Al_2O_3. Immersion test results determined effectiveness of barrier coatings and served as a guide for selection of a barrier for future application to fabricate a CuSiC MMC. Coated SiC rods were immersed in liquid Cu in order to measure the degree of Cu and SiC reaction. Uncoated α-SiC rods after exposure to liquid Cu at 1150°C for 30 min experienced Cu transport up to 500 μm depth into the SiC rods. All barrier coatings (TiN, TiN/TiC/TiCN/TiN, TiN/TiC/Al_2O_3 and Diamond-like Carbon) upon α-SiC rods decreased infiltration of Cu into SiC to less than 5 microns depth during immersion tests at 1150°C for 30 and 60 min.

2. Experimental

Coatings were applied to 7 mm diameter Hexoloy SA α-SiC rods, manufactured by Saint-Gobain (formerly Carborundum). Hexoloy SA α-SiC is a pressureless, sintered form of α-SiC, with a density greater than 98 percent theoretical. It has a fine grain size structure (8 microns) and contains no free silicon.

Rods with barrier coatings were inserted into machined high purity, low oxygen Cu (Gindre Duchavany CDA 101) (Fig. 1). Gindre Duchavany CDA 101 Cu was measured by glow discharge mass spectrometry (GDMS) and Leco combustion to be +99.996w% pure Cu on a metals basis with 11 ppmw oxygen. The rod and machined copper were placed into a POCO graphite crucible (Fig. 2). The crucible was covered

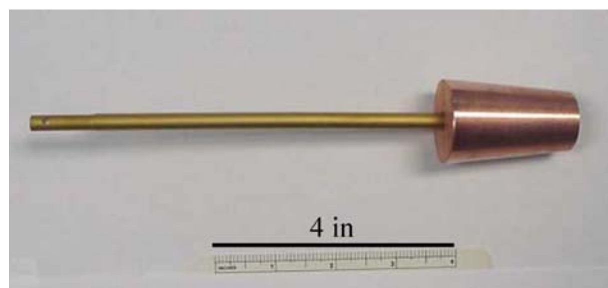

Figure 1 TiN/TiC/TiCN/TiN coated α-SiC rod inserted in machined high purity, low oxygen Cu.

Figure 2 CVD TiN/TiC/TiCN/TiN Coated α-SiC rod inserted in machined Cu placed inside graphite crucible.

with graphite foil to prevent contamination during heating and cooling from any airborne particulates and to further shield against oxygen. Each graphite crucible containing the copper with a coated α-SiC rod inside were placed inside a resistance heated vacuum furnace (Fig. 3). Tungsten wire was used to fix the rods in a near vertical position during the immersion in liquid copper. Temperature was increased at an average heating rate of 29°C/min to a maximum (soak) temperature of 1150°C. The ramp rate between 865°C and soak temperature averaged 12°C/min. Temperature was measured with an optical pyrometer by measurement of radiant energy emitted from the surface of the graphite crucible. The optical pyrometer was limited to a minimum detection limit of 865°C. After exposure to temperature for the desired time, power to the heating elements was turned off for a free cool to ambient. Glow discharge mass spectroscopy (GDMS) used to determine the chemical assay of the Cu specimens had a sub-ppm minimum detection limit with an experimental accuracy of ±20% for the reported concentration values.

Cooling rate between soak temperature and 865°C averaged 12°C/min. Although the time at maximum temperature is reported, it should be noted that the actual time at high temperature (above 865°C) was ∼37 min longer than the time referenced in the report due to the rate of heating and cooling. Rods were kept immersed in liquid copper during cooling to allow solidification of the copper in contact with the SiC rod. This facilitated simultaneous analysis of the rod and surrounding Cu after immersion by scanning electron microscopy (SEM) and energy dispersive X-ray spectroscopy (EDXS) analysis. PVD TiN coated SiC rods had the highest quality of all coatings prior to immersion, based upon uniformity of coating and good adherence (Fig. 4). The SEM micrograph and EDXS analysis of a cross-sectioned rod prior to immersion showed Ti rich spectra associated with the coating consistent with TiN (Fig. 5). The square in the center of the SEM micrographs marks the area of EDXS signal collection. The CVD TiN/TiC/TiCN/TiN

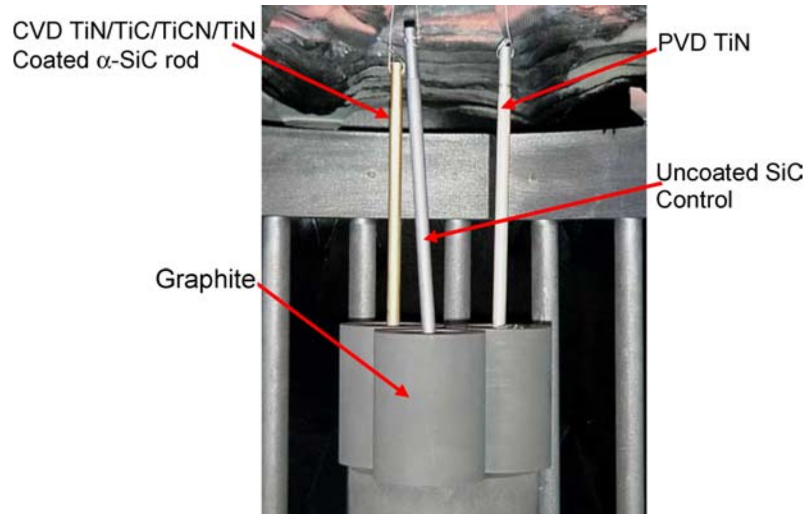

Figure 3 Immersion test crucibles and rods after heating to 1150°C for 30 min.

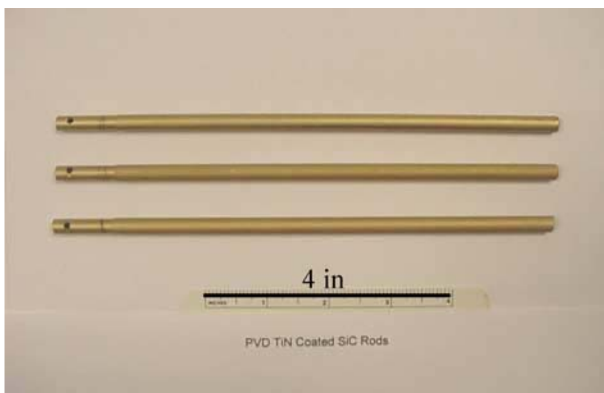

Figure 4 Photo image of PVD TiN Coated SiC Rods prior to immersion in liquid Cu.

coated SiC rods prior to immersion exhibited variable coating adherence as exhibited by areas with release of coating (spalls) on two of three rods (Fig. 6). The spalls were ~0.5 mm in size. SEM/EDS analysis of the TiN/TiC/TiCN/TiN multi-layered coating on a SiC rod exhibited the expected Ti rich EDS spectra (Fig. 7). The rod without visible spalls was used for immersion in liquid Cu at 1150°C for 30 min. The rod used for the 1150°C-60 min immersion test had spalls located on the end exposed to liquid Cu during immersion. The CVD TiN/TiC/Al_2O_3 coated SiC rods exhibited coating spalls on all three rods near the center, but no spalls were located on the end exposed to liquid Cu during immersion (Fig. 8). SEM/EDS analysis of the TiN/TiC/Al_2O_3 multi-layered coating on a SiC rod exhibited characteristic Ti and Al rich spectra (Fig. 9). The CVD diamond like carbon (DLC) coated SiC rods had incomplete coating coverage, spalling and a sooty appearance on the opposite end of the rod from the liquid Cu immersion (Fig. 10). SEM micrographs of the DLC coated SiC rods are shown in Fig. 11.

Thickness of coatings before and after immersion was determined by image analysis using the GAIA® software. The software is first calibrated according to the magnification of the image to be analyzed. The area of interest (AOI) is selected and the thickness of the coatings measured using measurement tools in the GAIA® software (GAIA Blue ver 5.0, Mirero Inc, Korea). Images taken from ten random areas were analyzed with 12 coating thickness measurements for each of the ten areas. Average and standard deviation was determined for all coating thickness measurements of a given coating.

Thermal conductivity measurements of Cu before and after immersion tests was determined from laser

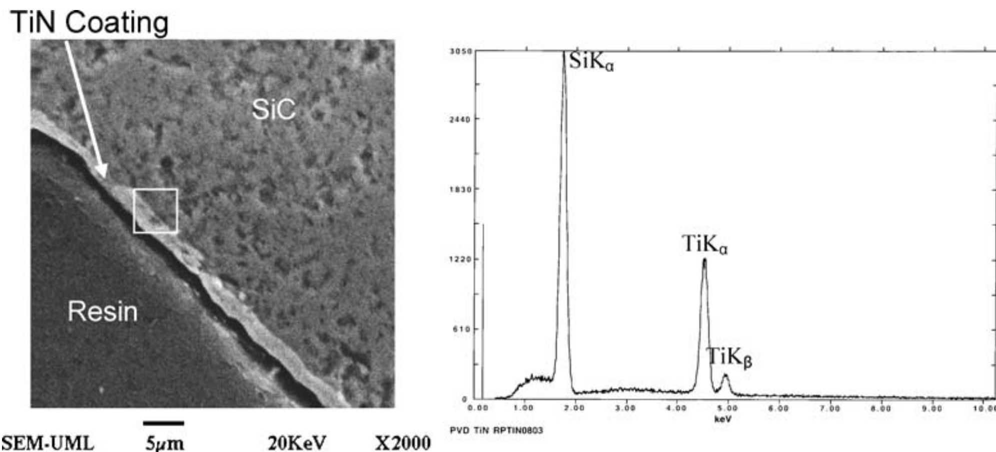

Figure 5 SEM photomicrograph and X-ray EDS spectra of a cross-sectioned PVD TiN coated SiC rod prior to immersion in liquid Cu.

Figure 6 Photo image of CVD TiN/TiC/TiCN/TiN Coated SiC Rods.

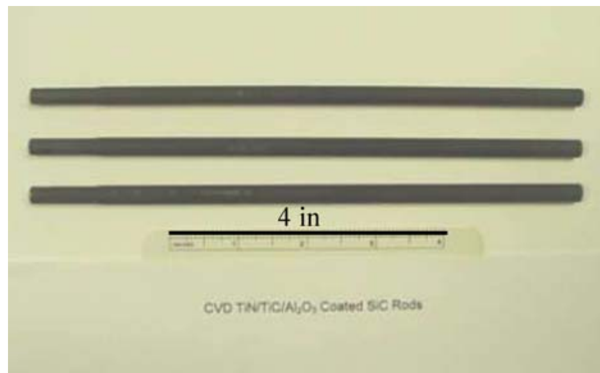

Figure 8 Photo image of CVD TiN/TiC/Al_2O_3 Coated SiC Rods.

flash thermal diffusivity measurement. The thermal conductivity values were had a measurement error of ±2% of the reported values.

3. Results and discussion

3.1. Presence of interfacial reactions between Cu and SiC

The presence of interfacial reactions was substantiated by SEM/EDXS analysis of the uncoated SiC rod after immersion into liquid Cu at 1150°C for 30 min. SEM micrographs after immersion show a reaction zone with significant Cu penetration of ∼500 μm depth into the uncoated SiC rod, labeled *Cu-SiC reaction zone* (Fig. 12). The initial SiC rod diameter prior to immersion is marked by the interface between the areas labeled *Cu* and *Cu-SiC reaction zone* in Fig. 12.

The formation of the CuSiC reaction zone has also been observed in the literature study by Z. An *et al.* who confirmed the presence of interfacial reaction at 850°C [11]. The liquid Cu reacted with the uncoated SiC rod resulting in decomposition of SiC as observed by transmission electron microscopy (TEM) of the Cu-SiC reaction zone (shown in Fig. 13a). The light and dark phases of the TEM image have been determined by electron diffraction to be crystalline copper silicide and copper carbide, respectively. The Cu-Si presence is in agreement with the literature which states that due to the strong Cu-Si interactions, dissolution of SiC occurs with the formation of Si and C dissolved into Cu [12]. The literature does not report crystalline Cu-C phase presence after reaction of SiC and Cu.

The amount of Si present in the Cu after immersion tests was determined by glow discharge mass spectroscopy (GDMS). The Si content in the copper prior to immersion of the uncoated SiC rod was 0.19 ppmw (parts per million on weight basis) and after immersion the Si content increased by more than 5 orders of magnitude to 1×10^4 ppmw (Table I). Decomposition of SiC in contact with Cu is the only source of additional Si which dissolved in the liquid Cu. The Cu thermal conductivity prior to immersion was measured at 387.0 W/mK and decreased by 66% to 128.5 W/mK after immersion as the Si content in the Cu increased to 1×10^4 ppmw. All Cu specimens were fully dense with no porosity detected. Contamination of Cu with small amounts of dissolved Si dramatically decreased thermal conductivity. It is clear that there was considerable reaction between the Cu and SiC phases. These reactions would be detrimental to the thermal properties of the fabricated CuSiC composite. The effectiveness of

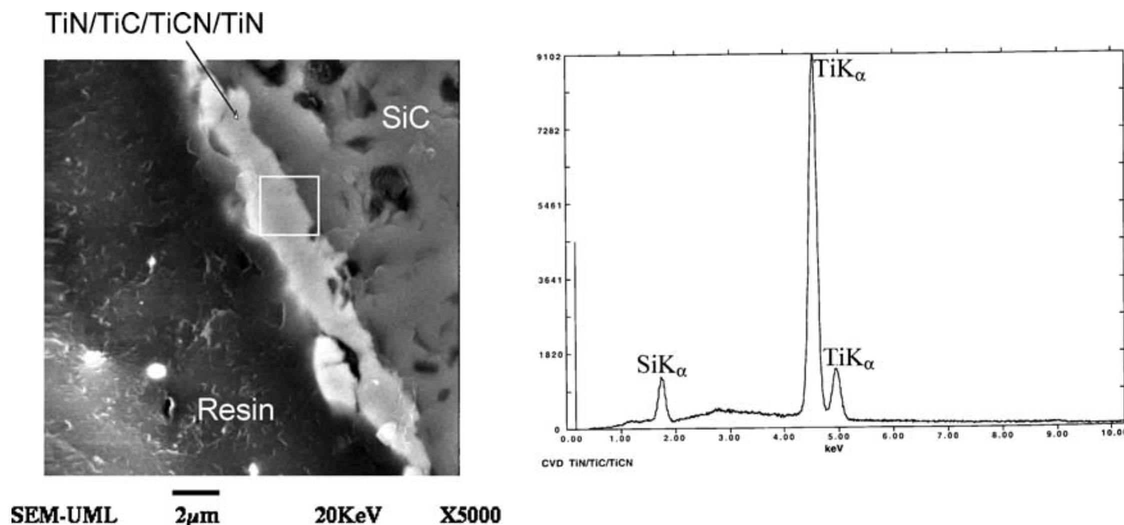

Figure 7 SEM photomicrograph and X-ray EDS spectra of a cross-sectioned CVD. TiN/TiC/TiCN/TiN coated SiC rod prior to immersion in liquid Cu.

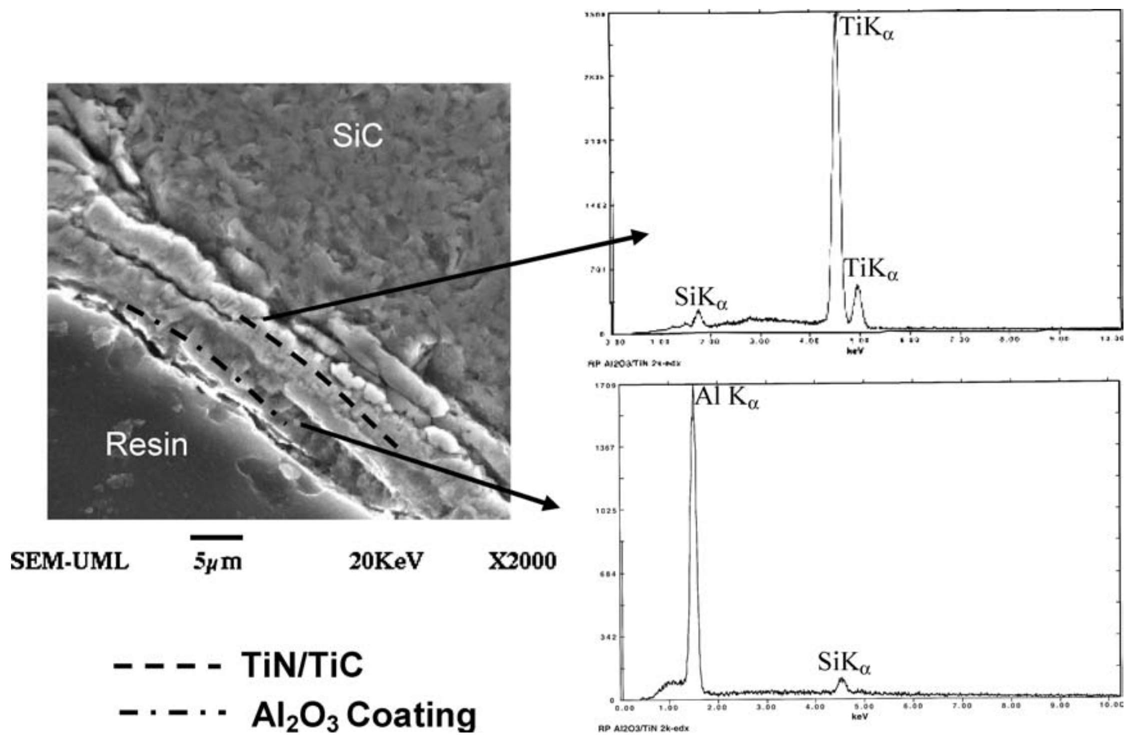

Figure 9 SEM photomicrograph and X-ray EDX spectra of a cross-sectioned CVD TiN/TiC/Al_2O_3 coated SiC rod prior to immersion in liquid Cu.

Figure 10 Photo image of CVD Diamond like Carbon Coated SiC Rods.

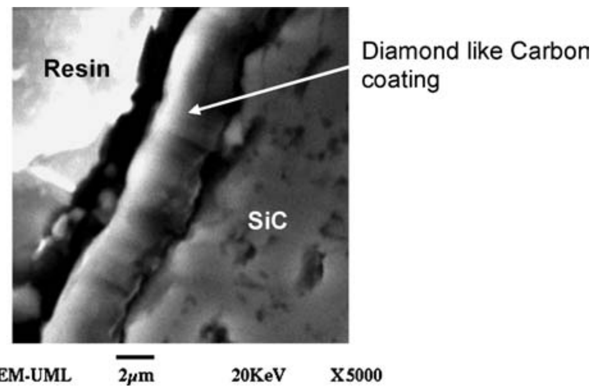

Figure 11 SEM photomicrograph of a cross-sectioned CVD Diamond like Carbon coated SiC rod prior to immersion in liquid Cu.

barrier coatings to passivate the Cu-SiC reaction was quantified in the following section.

3.2. Effectiveness of diffusion barriers between the Cu and SiC Systems

Several barrier coatings were applied to α-SiC rods, immersed in liquid copper and evaluated for effectiveness to prevent Cu transport to, and reaction with, SiC. The coatings were

- Physical Vapor deposited (PVD) TiN
- Chemical Vapor Deposited (CVD) TiN/TiC/TiCN/TiN multilayered coatings
- Chemical Vapor Deposited (CVD) TiN/TiC/Al_2O_3 multilayered coatings
- Chemical Vapor Deposited (CVD) Diamond-like Carbon

TABLE I Thermal conductivity as a function of silicon content of Cu before and after immersion of coated and uncoated SiC rods

Copper	Thermal conductivity (W/m-K)	Total impurities (ppmw)	Si (ppmw)
As-received	387.0	32	0.19
Post immersion			
1150°C, 30 min	216	227	198
1150°C, 60 min	233	1,125	1,100
1160°C, 75 min	128.5	10,058	10,000

The first series of coated rod immersion tests in liquid Cu were performed at 1150°C for 30 min. The TiN coating prevented Cu transport to the SiC rod as determined by SEM/EDS analysis of Cu/PVD TiN coated SiC rod cross-sections after immersion (Fig. 14). A distinct, well defined interface was exhibited between Cu and the PVD TiN coated SiC rod in the secondary electron image (SEI). EDS X-ray maps of Cu and Si show areas rich in these elements as brighter colored regions.

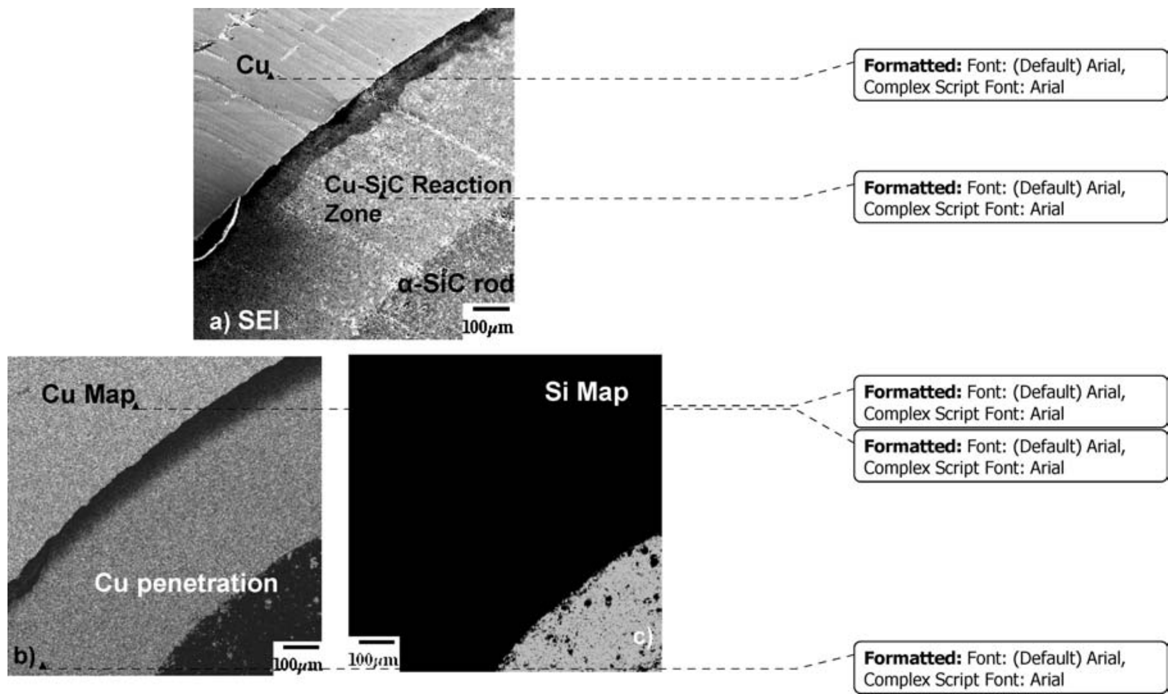

Figure 12 Cross-section of the α-SiC rod after immersion in liquid Cu at 1150°C for 30 min. (a) SEM image showing the reaction zone of Cu and SiC (b) and (c) Energy dispersive X-ray maps of Cu and Si respectively.

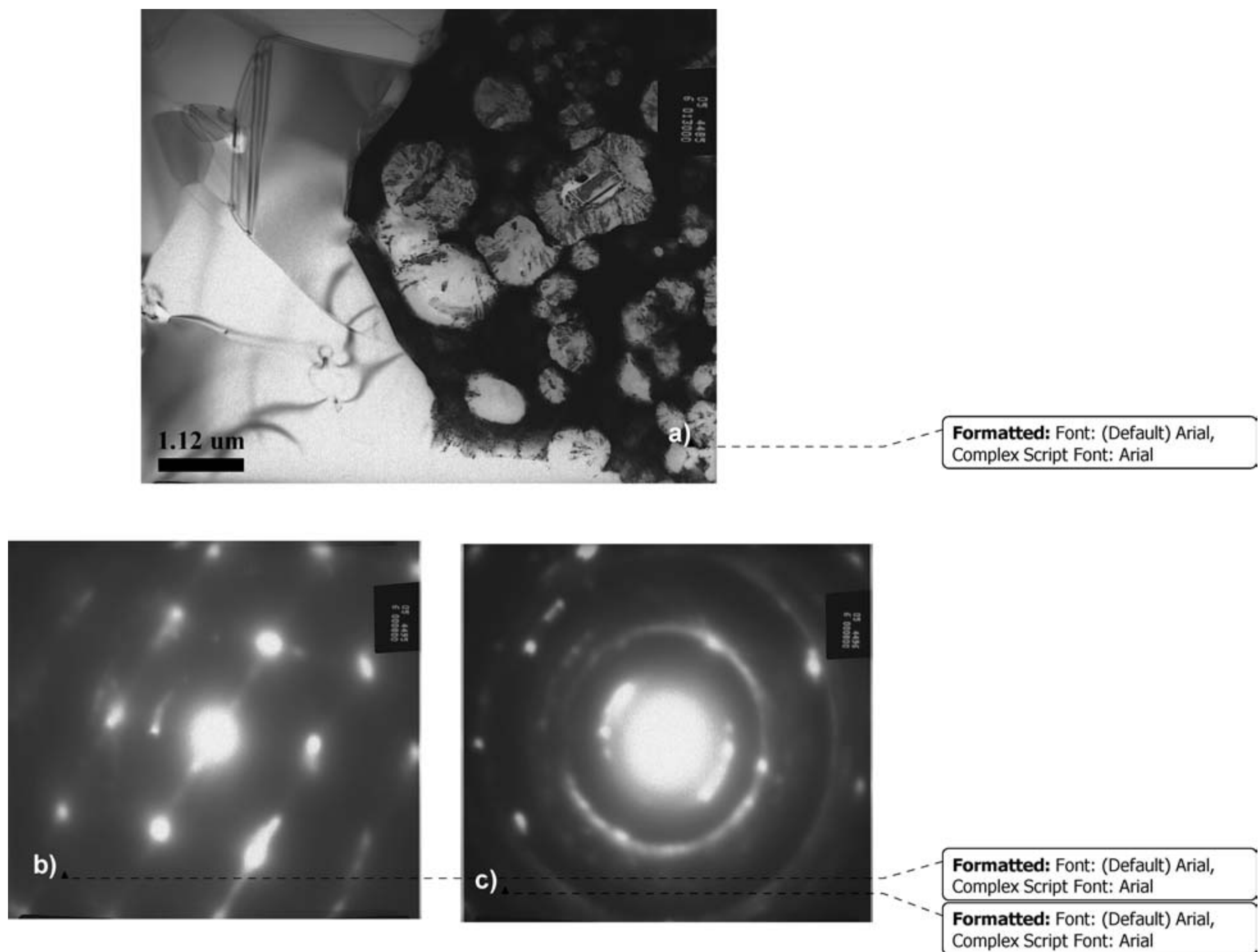

Figure 13 (a) TEM of Cu/SiC reaction zone showing the bright field image of the Cu-C and Cu-Si phases. (b) Electron diffraction pattern of the Cu-Si phase and (c) Electron diffraction of the Cu-C phase.

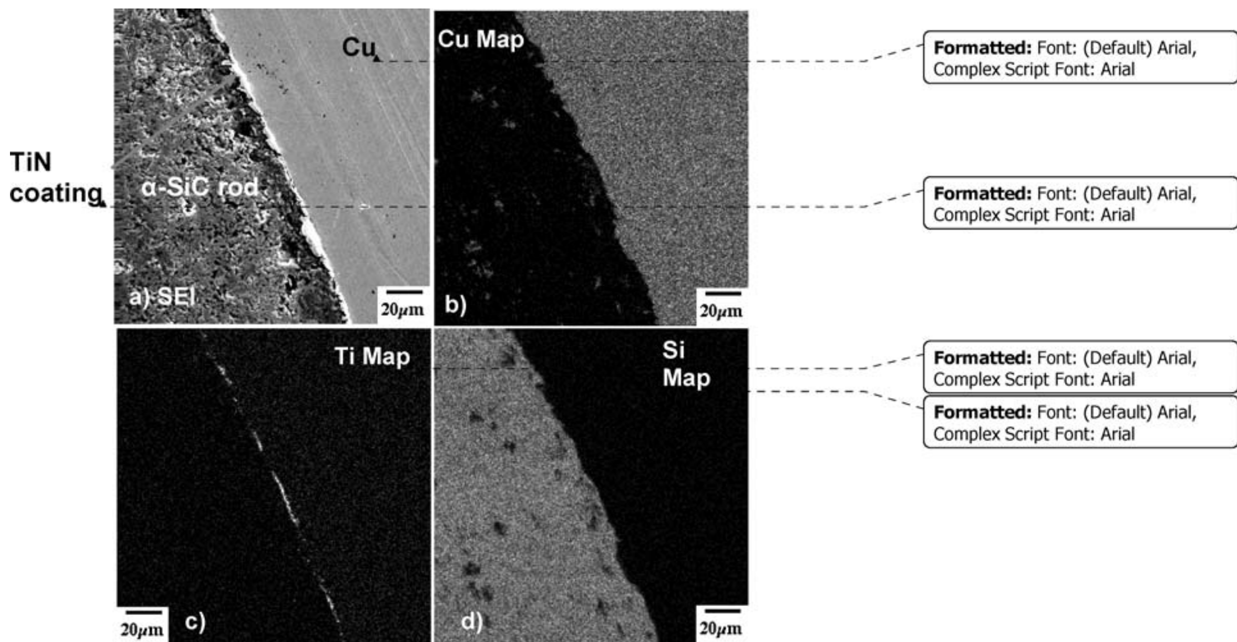

Figure 14 SEM/EDS analysis of a cross-sectioned PVD TiN coated α-SiC rod after immersion in liquid Cu at 1150°C for 30 min. (a) Secondary electron image (SEI) (b)–(d) X-ray maps.

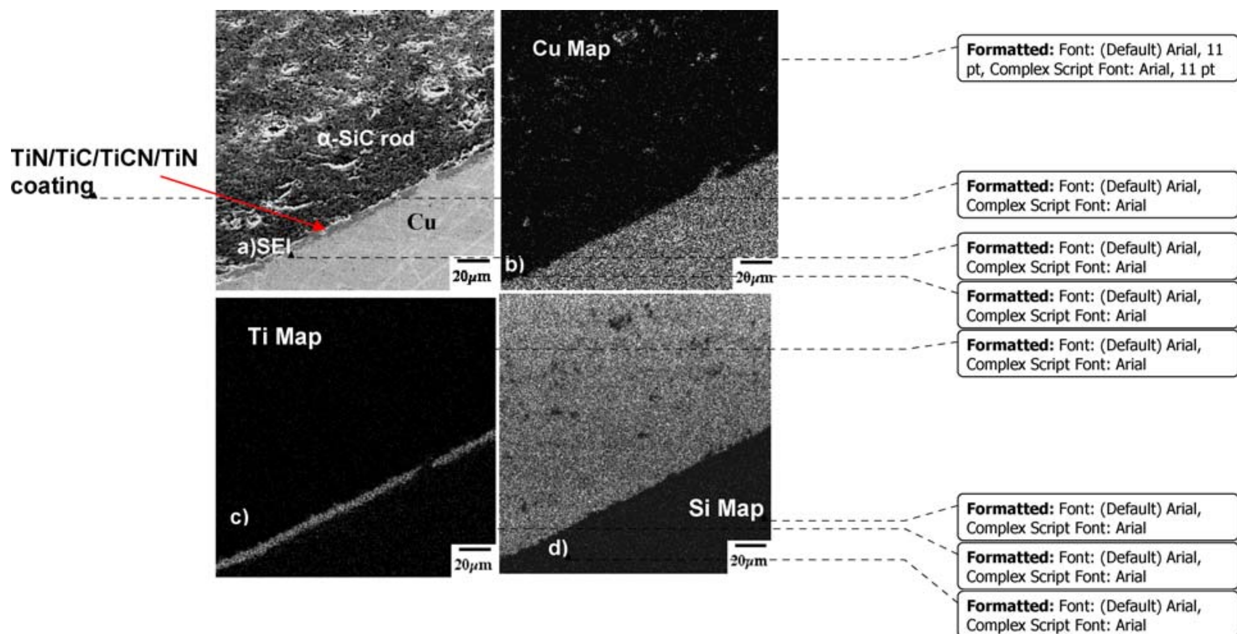

Figure 15 SEM/EDS analysis of a cross-sectioned CVD TiN/TiC/TiCN/TiN coated α-SiC rod after immersion in liquid Cu at 1150°C for 30 min. (a) Secondary electron image (SEI) (b)–(d) X-ray maps.

The Cu and Si rich regions were separated by a Ti rich region (the TiN coating). There was no evidence of Cu transport into the SiC rod or a Cu-SiC reaction zone as was apparent for the uncoated SiC control rods immersed in liquid Cu for 30 min at 1150°C (Fig. 12).

The SEM/EDS analysis of CVD TiN/TiC/TiCN/TiN multilayered coated SiC after immersion for 30 min at 1150°C in liquid Cu also showed no penetration of Cu into SiC and no apparent evidence of Cu-Si interdiffusion (Fig. 15). There was a clear distinct interface between the Cu and SiC regions demonstrating effectiveness of the TiN/TiC/TiCN/TiN multi-layer coating as a diffusion barrier. CVD TiN/TiC/Al_2O_3 coating also maintained its integrity and prevented Cu-Si interdiffusion at 1150°C in liquid Cu for 30 min (Fig. 16). The Al_2O_3 coating layer exhibited an apparent reduction of thickness possibly as a result of dissolving in the liquid Cu. SEM micrographs of the DLC coated SiC rods are shown in Fig. 17. SEM/EDS analysis of CVD DLC coated SiC rod after immersion for 30 min at 1150°C in liquid Cu showed a small degree of Cu penetration into SiC resulting from Cu-Si interdiffusion (Fig. 17b). The DLC coating was difficult to detect after immersion in liquid Cu. DLC coatings used may have not been stable under immersion conditions. The hydrogen content of the DLC coating was not known, however most DLC coatings contain hydrogen in varying degrees captured within the amorphous structure

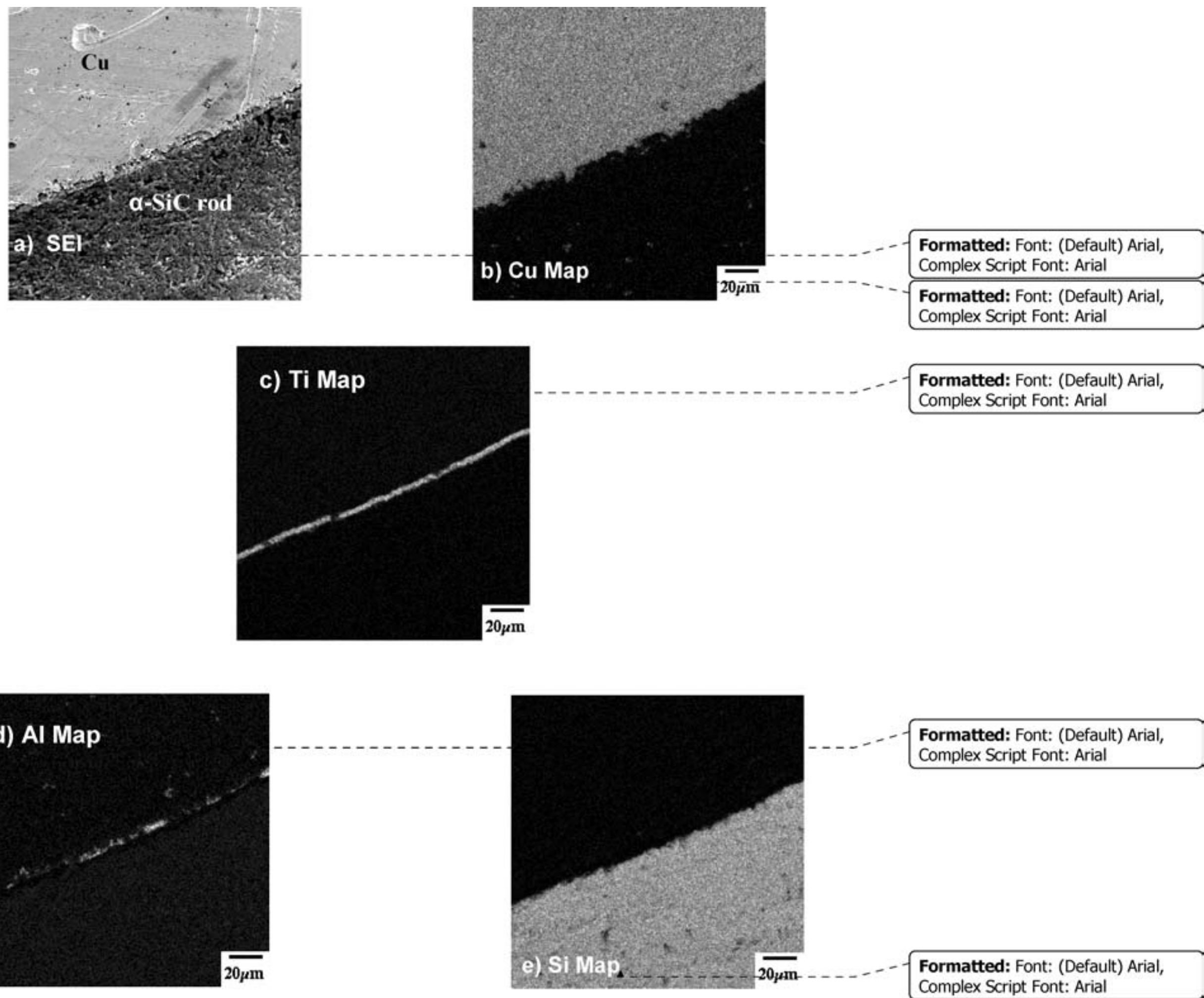

Figure 16 SEM/EDS analysis of a cross-sectioned CVD TiN/TiC/Al_2O_3 coated α-SiC rod after immersion in liquid Cu at 1150°C for 30 min. (a) Secondary electron image (SEI) (b)–(e) X-ray maps.

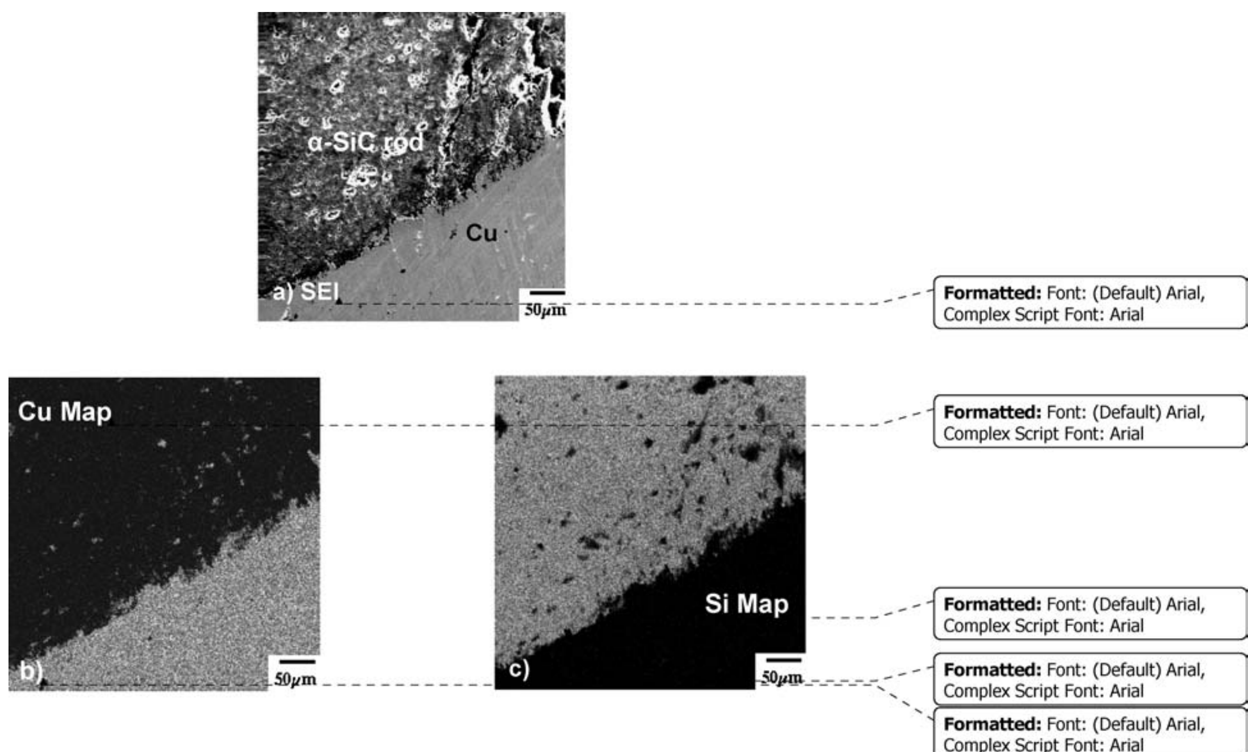

Figure 17 SEM/EDS analysis of a cross-sectioned CVD Diamond Like Carbon (DLC) coated α-SiC rod after immersion in liquid Cu at 1150°C for 30 min. (a) Secondary electron image (SEI) (b)–(c) X-ray maps.

as a by-product of the deposition reaction which leads to chemical instability at temperatures below 1000°C. (15) Instability of the DLC coating combined with the dissolution/precipitation mechanism proposed by Rado *et al.* (12) could explain why the DLC coating was apparently removed during immersion in liquid Cu. The carbon from the potentially unstable DLC would be locally soluble up to the solubility limit for C in Cu which is in the ppm range at 1150°C. Subsequent formation of crystalline graphitic or amorphous carbon by precipitation would allow additional DLC to dissolve to facilitate removal of the DLC coating.

It was observed that the multilayer barriers of TiN/TiC/TiCN/TiN and TiN/TiC/Al_2O_3 remained intact at the Cu/SiC interface following immersion in liquid Cu (Figs 15 and 16). Both coatings effectively passivated the interfacial reaction between Cu and SiC. The single layered coatings of PVD TiN and CVD DLC also decreased interfacial reaction between Cu and SiC, but an appreciable amount of these coatings was removed during immersion tests. DLC coatings were almost entirely removed during immersion in liquid Cu. The TiN coatings prior to immersion in liquid copper were of consistent thickness (Fig. 5), but after immersion in liquid Cu the TiN coatings were of decreased and highly variable thickness (Fig. 14). The stability of the barriers to withstand high temperatures for longer periods of time is critical for protection of the SiC during hot pressing or casting CuSiC metal matrix composites. Hence, immersion tests were also conducted at 1150°C for a longer 60 min exposure, after which retained coating coverage was quantified.

3.3. Determination of the most effective barrier

The effectiveness of the barriers was determined by measuring the thickness of the coatings before and after immersion tests, and coating coverage on the SiC rod after immersion, at 1150°C for 30 and 60 min (Tables II and III). The multilayered coatings of TiN/TiC/TiCN/TiN and TiN/TiC/Al_2O_3 had the least change in coating thickness and the most post-immersion coverage after the 1150° C-30 min immersion in liquid Cu (Table II). The TiN/TiC/TiCN/TiN coating had statistically insignificant loss of coating thickness and maintained greater than 95% coverage after the 30 min. immersion. The TiN/TiC/Al_2O_3 coating lost 1 μm thickness, but maintained significantly greater coverage at >75% compared with the TiN and DLC coatings which retained only 25 and 5% coverage, respectively, after the 1150°C-30 min immersion in liquid Cu. It was not meaningful to measure the coverage for the TiN/TiC/TiCN/TiN coatings after the 1150°C-60 min immersion in liquid Cu due to separation of the coating from the SiC rod after immersion. Note that the TiN/TiC/TiCN/TiN coatings used for the1150°C-60 min immersion had poor adhesion as exhibited by coating spalls prior to immersion tests on the end of the SiC rod exposed to liquid Cu. These coatings did prevent Cu transport into the SiC rod despite the poor adherence, but most of the TiN/TiC/TiCN/TiN coating separated from the SiC rod making assessment of coverage dubious (Table III). The TiN/TiC/Al_2O_3 coatings prevented ingress of Cu into the SiC rods after 60 min immersion in liquid Cu at 1150°C, although appreciable coating thickness loss was noted. The coating coverage was 70–80% after immersion for the TiN/Al_2O_3 coating. The TiN coating was mostly removed after immersion in liquid Cu for 60 min at 1150°C and Cu transport into the SiC rod was noted. These results are consistent with the literature which supported superiority of the multilayered coatings over the single layered barrier coatings from disruption of rapid diffusion paths along the epitaxially grown grain boundaries by multiple coating/coating interfaces [13, 14]. Coating thickness prior to immersion at 1150°C-60 min for the TiN/TiC/TiCN/TiN and TiN/TiC/Al_2O_3 coatings were 78 and 49% larger, respectively, as compared with the 30 min immersion (Table III). This was the result of unintentional process variability by the coating vendor. This may also be the cause for lower adherence due to expected increase of expansion mismatch stress caused by the thicker

TABLE II Coating thickness before and after immersion test at 1150°C for 30 min and the area % coverage of the coatings on the SiC rods after immersion

Coating	Mean thickness before immersion (μm)	Mean thickness after immersion	Area % coverage after immersion (%)
TiN/TiC/TiCN/TiN	4.65	4.35 μm	>95
TiN/TiC/Al_2O_3	6.25	5.17 μm	75–80
TiN	2.17	1.66 μm	20–25
DLC	2.91	Barrier mostly absent	5

TABLE III Coating thickness before and after immersion test at 1150°C for 60 min and the area % coverage of the coatings on the SiC rods after immersion

Coating	Mean thickness before Immersion (μm)	Mean thickness after immersion (μm)	Area % Coverage after immersion
TiN/TiC/TiCN/TiN	8.27	4.70	Adherence failure
TiN/TiC/Al_2O_3	9.3	5.5	75–80 %
TiN	4.68	1.66	20–25%

TABLE IV Silicon concentration in Cu after immersion of the bare and coated SiC rods at 1150°C for 30 and 60 min

SiC rod description	Time at temperature (mins)	Si concentration (ppmw)
Uncoated SiC	30	198
	60	1100
TiN/TiC/TiCN/TiN	30	0.39
	60	0.5
TiN/TiC/Al_2O_3	30	0.24
	60	0.95
TiN	30	44
	60	23
Diamond like carbon	30	104
	60	102

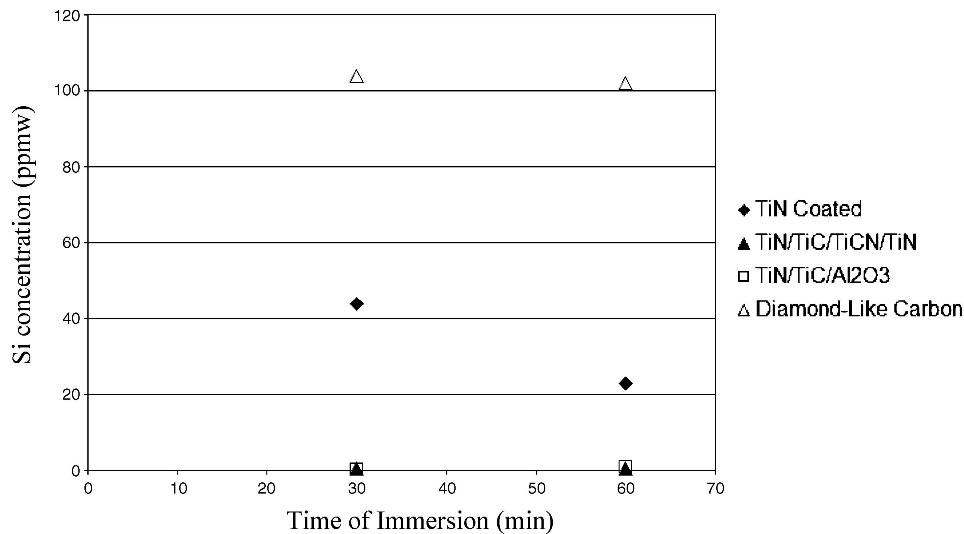

Figure 18 Silicon concentration in Cu by GDMS after immersion of coated and uncoated rods at 1150°C for 30 and 60 min.

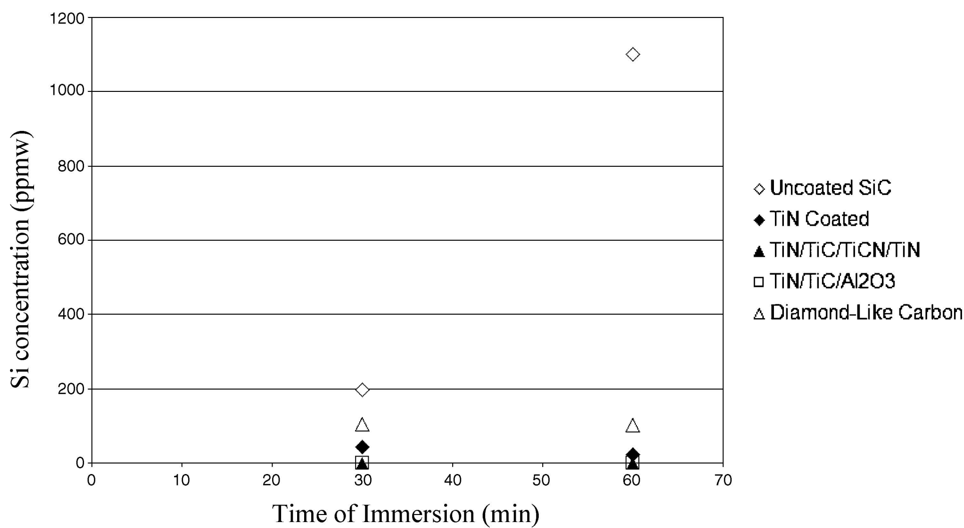

Figure 19 Silicon concentration in Cu by GDMS after immersion of coated rods at 1150°C for 30 and 60 min.

coatings. Table IV and Fig. 18 provide a comparison between Si concentration in Cu after the immersion of bare and coated α-SiC rods in liquid Cu. The Si concentration in Cu after the 1150°C-60 min immersions was 0.39 and 0.24 ppmw for TiN/TiC/TiCN/TiN and TiN/TiC/Al_2O_3 multi-layered coatings, respectively, on SiC rods . The Si concentration in Cu after the 1150° C-30 min immersions was 44 and 104 ppmw for TiN and DLC coatings, respectively, on SiC rods. Fig. 19 illustrates the superiority of the multi-layered coatings of TiN/TiC/TiCN/TiN and TiN/TiC/Al_2O_3 by comparing the Si concentration in the Cu after the immersion at 1150°C for 30 and 60 min. The Cu had excellent thermal conductivities of +390 W/mK after immersion with the coated rods (Table V). An interesting observation was that even the single layered PVD TiN barrier coating protected SiC from Cu to achieve high thermal conductivity of the Cu. This is an important result since practical methods to coat SiC powders to make CuSiC MMC's were initially constrained to simple, single layered coatings.

TABLE V Thermal conductivity of Cu after immersion of coated SiC rods at 1150°C for 30 and 60 min

Coating	Immersion time (min)	Si in Cu (ppmw)	*k* of Cu (W/mK)
Bare SiC	60	1100	233
TiN	60	23	391.85
TiN/TiC/TiCN/TiN	60	0.50	401.3
TiN/TiC/Al_2O_3	60	0.95	390.25
DLC	60	102	379.25

4. Conclusions

Highly pure α-SiC rods without a barrier coating will react with high purity liquid Cu at temperatures between 1050 to 1150°C. Si concentration increase in Cu after exposure of SiC to liquid Cu at 1150°C for 30 min caused pure Cu to have a significant increase in Si concentration from 0.19 ppm to 1×10^4 ppm with an attendant drop in thermal conductivity from 387 to 129 W/mK. The multilayer coatings of CVD TiN/TiC/TiCN/TiN and CVD TiN/TiC/Al_2O_3 proved to be more effective to passivate the SiC-Cu reaction up to 1150° C for 60 min by serving as a better barrier to

liquid Cu transport than the single layer CVD Diamond like carbon coatings and PVD TiN coatings. Passivation coatings prevented Cu-SiC reaction at 1150°C for 60 min to retain Cu conductivity of greater than 390 W/mK.

Acknowledgements
The authors would like to thank Q-Matrix for sponsoring this work, industry partners: Powdermet, Ritcher Precision, Federal Technology Group, Ceracon, Wright Patterson Air Force Lab for raw material supplies, Northern Analytical for chemistry analysis and Dr. Rudy Enck for the thermal flash diffusivity measurements. Special acknowledgement is due to Mr. Rob Hay for technical support and encouragement.

References
1. S. SESHAN, A. GURUPRASAD, M. PRABHA and A. SUDHAKAR, *J. Ind. Inst. Sci.* **76** (1996) 1.
2. M. TAN, Q. XIN, Z. LI and B. Y. ZONG, *J. Mater. Sci.* **36** (2001) 2045.
3. P. MOLDOVAN, *UPB Sci. Bull. Series B: Chem. Mater. Sci.* **61** (1999) 117.
4. S. SASTRY, M. KRISHNA and J. UCHIL, *J. Mater. Engng. Perform.* **10** (2001) 220.
5. C. A. CHANG, *J. Appl. Phys.* **67** (1990) 556.
6. S. Y. JANG, S. M. LEE and H. K. BAIK, *J. Mater. Sci: Mater. Electron. Soc.* **7** (1991) 271.
7. C. A. CHANG, *J. Appl. Phys.* **67** (1990) 6184.
8. S. Q. WANG, I. RAAIJMAKERS, B. J. BURROW, S. SUTHER, S. REDKAR and K. B. KIM, *ibid.* **68** (1990) 5176.
9. K. HOLLOWAY, P. M. FRYER, C. CABRAL, JR., J. M. E. HARPER, P. J. BAILEY and K. H. KELLEHER, *ibid.* **71** (1992) 5433.
10. S. Q. WANG, S. SUTHER, B. J. BURROW and C. HOEFLICH, *ibid.* **73** (1993) 2301.
11. Z. AN, *et al.*, *Appl. Sur. Sci.* **216** (2003) 169.
12. C. RADO, *et al.*, *Acta Mater.* **48** (2000) 4483.
13. Y. T. KIM, *et al., Thin Solid Films* **347** (1999) 214.
14. K. M. LATT, *et al.*, *Mater. Sci. Engng.* **B84** (2001) 217.
15. R. HAY, personal correspondence, CPS Corporation, Chartley, MA, September 2004.

Received 10 November 2004
and accepted 12 January 2005